DEDICATED TO THE MEMORY OF
Associated Professor MARIUS IULIU SALAJAN (1952-2004)

THE EFFECT OF GOLD NANOPARTICLES SYNTHESIZED BY SODIUM CITRATE AND FUNCTIONALIZED WITH ANTICANCER AND NATURAL COMPOUNDS ON CANCER CELL LINES

Madalina Anca UJICA[a], Ionel MANG[a,b] [iD], Ossi HOROVITZ[a*] [iD],

Olga SORITAU[c] [iD], Gheorghe TOMOAIA[b,d] [iD], Aurora MOCANU[a] [iD],

Horea-Rares-Ciprian BENEA[b] [iD], Viorica RAISCHI[a,e] [iD],

Csaba VARHELYI[a] [iD], George BORODI[f] [iD],

Maria TOMOAIA-COTISEL[a,d*] [iD]

ABSTRACT. Natural compounds, such as trans-resveratrol, R, piperine, P, and icariin, Ic, have antioxidant and anti-inflammatory properties, and potential anticancer activity. Gold nanoparticles, GNPs, are biocompatible and can be used as carriers for biomolecule delivery, improving their performance at a small dose. The aim of the present study was to synthesize GNPs with sodium citrate, noted GNP_C (or GNP-C), and enhancing their stability and anticancer activity by functionalization with R, P, Ic, asparagine, A, and doxorubicin, D, as a

[a] *Babeş-Bolyai University, Research Center of Excellence in Physical Chemistry, Faculty of Chemistry and Chemical Engineering, 11 Arany Janos Str., RO-400028, Cluj-Napoca, Romania*
[b] *Department of Orthopedics and Traumatology, Iuliu Hatieganu University of Medicine and Pharmacy, 47 General Traian Moşoiu Str., RO-400132, Cluj-Napoca, Romania*
[c] *Oncologic Institute Prof. Dr. I. Chiricuţă, 20-26 Republicii Str., 400015 Cluj-Napoca, Romania*
[d] *Academy of Romanian Scientists, 3 Ilfov Str., RO-050044, Bucharest, Romania*
[e] *Institute of Physiology and Sanocreatology, State University of Moldova, Academy 1 Str., MD-2028, Chișinău, Moldova*
[f] *National Research-Development Institute for Isotopic and Molecular Technologies, 67-103 Donath Str., RO-400293, Cluj-Napoca, Romania.*
[*] *Corresponding authors: mcotisel@gmail.com, ossihor@yahoo.com*

M. A. UJICA, I. MANG, O. HOROVITZ, O. SORITAU, GH. TOMOAIA, A. MOCANU, H. R. C. BENEA,
V. RAISCHI, CS. VARHELYI, G. BORODI, M. TOMOAIA-COTISEL

standard drug. The obtained GNPs as cores, loading selected biomolecules, adsorbed on their surface as shells, were characterized by various methods, UV-Vis spectroscopy, XRD, AFM, TEM, and particle size analysis. The anticancer activity of functionalized GNP_C was evaluated using MTT assay in four human cell lines: breast cancer, MDA-MB-231 and MCF-7 cell lines, tumor stem cells (isolated from glioblastoma), a GM1 cell line, and a normal (healthy) stem cell line derived from a dental follicle, DF. GNP_C functionalized with R, P or Ic exhibited an anticancer activity comparable to GNP_C functionalized with doxorubicin for low concentrations in gold and in natural compounds, thus reducing side effects of anticancer drug. These promising results need further examination using various cell lines and animal models, to clinical applications.

Keywords: *functionalized gold nanoparticles, cytotoxicity and anticancer activity, cancer cell lines*

INTRODUCTION

Cancer is the second cause of death on Earth and requires a prompt identification (early cancer detection) and an efficient anti-cancer therapy [1]. The conventional chemotherapy and radiotherapy usually suffer from systemic toxicity. Moreover, cancer reappearance is too common, for example, in bone recurrence. Although huge efforts have been made, optimum treatment has not been achieved owing to the resistance of cancer cells to therapeutic treatment.

To overcome these difficulties, new biocompatible materials, like gold nanoparticles, GNPs, functionalized with anti-cancer drugs, have been developed as nanocarriers to kill cancer cells [2]. Gold nanoparticles can be synthesized by a variety of methods usually starting from tetrachloroauric acid as a precursor agent and using as a reducing agent either chemical substances, such as trisodium citrate, resveratrol and sodium borohydride, or plant extracts and microorganisms.

The typical synthesis of GNPs is the best known, which involves the chemical reduction of Au^{3+} ions from tetrachloroaurate to Au^0 atoms. This can only take place in the presence of a reducing agent, an agent that can sometimes also play the role of a stabilizing agent [2, 3]. This type of synthesis is well known since 1951, when Turkevich performed the first chemical synthesis of GNPs from a solution of chloroauric acid and sodium citrate [2, 4]. Although time has passed and many other reducing agents have been discovered, such as resveratrol, which creates a protective corona around the gold nanoparticle that not only stabilizes, but also potentiates the cytotoxic effect of GNPs in the fight against cancer cells [5]; however, the classic combination is still used.

Over time, scientists have developed and improved the classic synthesis method with the aim of better controlling the size and stability of the gold nanoparticles obtained. These changes mainly consist in varying the reaction conditions (temperature, pH, reaction time) or the concentrations of the reducing agent or the precursor [6]. In some cases, in addition to trisodium citrate, other substances are added, such as polyvinyl alcohol [7], carboxymethyl cellulose [8] or tannic acid [9, 10] with a role in directing the shape of the nanoparticle and co-encapsulation. In addition to chemicals, synthesis can also be aided by gamma ray irradiation [11]. Theoretical study [9] on the synthesis of GNPs, together with laboratory experiments, demonstrated that the variation of the reaction conditions helps control the synthesis of GNPs. Finally, it is demonstrated that anions of citrate are adsorbed on the surface of gold nanoparticles, GNP_C, through the central carboxylate groups [12].

Characterization methods play a very important role in establishing the efficiency of the synthesis. Thus, a variety of analysis methods are used, some of which we will review. UV-VIS spectroscopy shows the formation of the GNPs. [13, 14] Details on the formation of self-assembled layers on the surface of GNPs can be determined by TEM [15]. XRD confirms the crystalline nature of the nanoparticles of gold [16], and AFM reveals the morphology of GNPs self-assemblies. Besides these, other characterization techniques are also used, such as: FTIR, HR-TEM, SEM, Zeta potential and DLS.

To measure the effectiveness of GNP_C in cancer treatment, usually this is compared to the total inhibitor concentration that can reduce the cell viability with 50%, called IC50 [17]. Thus, over time, the cytotoxicity of GNP_C has been tested both on healthy cell lines, like BHK, L929 (fibroblasts), HDMEC (human dermal microvascular endothelial cell line) and hCMEC-D3 (human cerebral microvascular endothelial cells) [17-19] and on cancerous cell line, such as HeLa against healthy BHK cell line [18] and the results are somewhat agreeable. Other cancer lines [20-25] sensitive to gold nanoparticles synthesized with citrate were also used, for instance, ovarian carcinoma cell line [20]) and human lung adenocarcinoma cell lines [23]. In the case of breast cancer cell lines [24, 25], of interest to us in this work are MCF-7 and MDA-MB-231 cell lines; the literature data show that there is an anticancer activity of GNP_C, but at rather high concentrations [25]. This made us determined to find the right functionalization of GNP_C to increase cytotoxicity, but lowering the dose of therapeutic drug, for example doxorubicin. In addition to high toxicity for cancer cells, the substances used in treatments must be biocompatible with healthy cells, and fortunately, GNP_C are toxic to these only at high concentrations [7, 26-29].

As a novelty in this study, the anticancer activity of GNP_C was extended for the first time towards their functionalization with different natural biomolecules, namely resveratrol, piperine or icariin in comparison with doxorubicin, a standard anti-cancer drug.

Trans resveratrol, R, is a polyphenol produced by plants, and can form complexes with GNPs, whose biocompatibility has been demonstrated, making it a good candidate for drug potentiation [30-33]. Even alone, R has a slight anticancer action and it reduces cellular oxidative stress and inflammation [5, 34].

Piperine, an alkaloid obtained by extraction from *Piper longum* and *Piper nigrum,* whose properties have been used by medicine for a long time [35] for its antioxidant, anti-inflammatory and immunomodulatory effects; its anticancer ability leads to a sensitization of cancer cells increasing cell death by apoptosis [5].

Icariin, the main active ingredient in a Chinese anti-inflammatory drug, which once ingested is mostly transformed into its metabolite – icaritin – [36], and it is presented [37, 38] as an active participant in the increased intracellular accumulation of doxorubicin in human multidrug-resistant osteosarcoma cells.

In accordance with the properties of icariin, piperine and resveratrol, these compounds are used to make innovative complexes with GNP_C, which are further used in two breast cancer (MDA-MB 231 and MCF-7) cell lines and on tumor stem cells derived from glioblastoma: GM1. Glioblastoma multiform stem cells have a high proliferative potential, despite chemotherapy and irradiation, and they have the ability to form spheroids in suspension [39]. MCF-7 cells retain several characteristics of differentiated mammary epithelium, including the cytoplasmic estrogen receptor. The commonly studied triple negative breast cancer (TNBC) MDA-MB-231 cell line was established in the 1970s from pleural effusion of a breast cancer patient. This cell line has the advantage of being a source of breast tumor cells with high viability and proliferation ability [40].

The growing interest in nanotechnology for increasing the clinical efficacy of natural products, is justified by necessity to increase the bioavailability of bio-active compounds, improving the biomolecule stability within biological systems and increasing the solubility and transport across biological membranes of these compounds [41-43]. Phytochemicals (e.g., resveratrol) adsorbed onto gold nanoparticles had an enhanced bioactivity against cancer, leading to an increased cellular uptake and anti-cancer activity compared to the phytochemicals alone [43].

Based on the above, the goal of our study is centered on the activity of gold nanoparticles synthesized with citrate, GNP_C, and functionalized with natural substances, resveratrol, piperine or icariin to be an innovation in anticancer research.

RESULTS AND DISCUSSION

Gold nanoparticles synthesis, functionalization and characterization

Gold nanoparticles were prepared by reduction of a tetrachloroauric acid ($HAuCl_4$), solution with a trisodium citrate ($Na_3C_6H_5O_7$) aqueous solution. The obtained nanoparticles were denoted as GNP_C. The calculated gold content in the obtained colloidal solution was $0.6 \cdot 10^{-3}$ M (118 mg/L Au). The presence of GNP_C in the final solution was revealed by the red color, due to the SPR absorption band of gold nanoparticles. The band appears in the visible range of the UV-Vis spectrum, with a maximum at 531 nm wavelength. Their spectrum is compared with that of gold nanoparticles obtained by reduction with resveratrol (GNP_R) [44] (Au content 179 mg/L) in Figure 1.
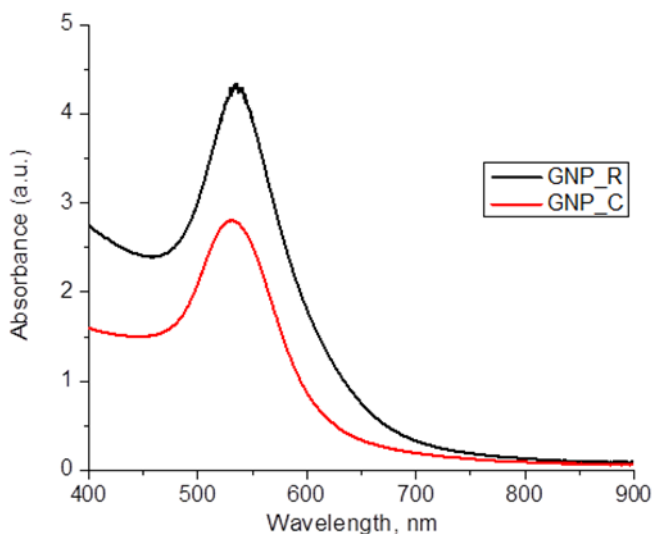

Figure 1. Comparison of UV-Vis (optical) spectra of GNPs solutions obtained by reduction with resveratrol (GNP_R) and with sodium citrate (GNP_C)

In Figure 2A, a TEM image for GNP_C is presented, and every nanoparticle is very well shown. From the diameters of a large number of GNPs (several hundred) measured in different TEM images for each sample, the histogram of size distribution in Figure 2B was obtained. The average diameter of synthesized GNP_C nanoparticles is 29.2 ± 4.8 nm.

The ξ-potential value measured on GNP_C is -31.5 mV, thus a stabilization by electrostatic repulsion can be assumed for their colloidal solution. The threshold value assuring electrostatic stability is considered to

be ±30 mV [45]. The average diameter of particles measured by DLS is 31.64 nm, only slightly bigger than the diameter estimated from the TEM images. This suggests the presence of a rather thin organic coating of GNPs.
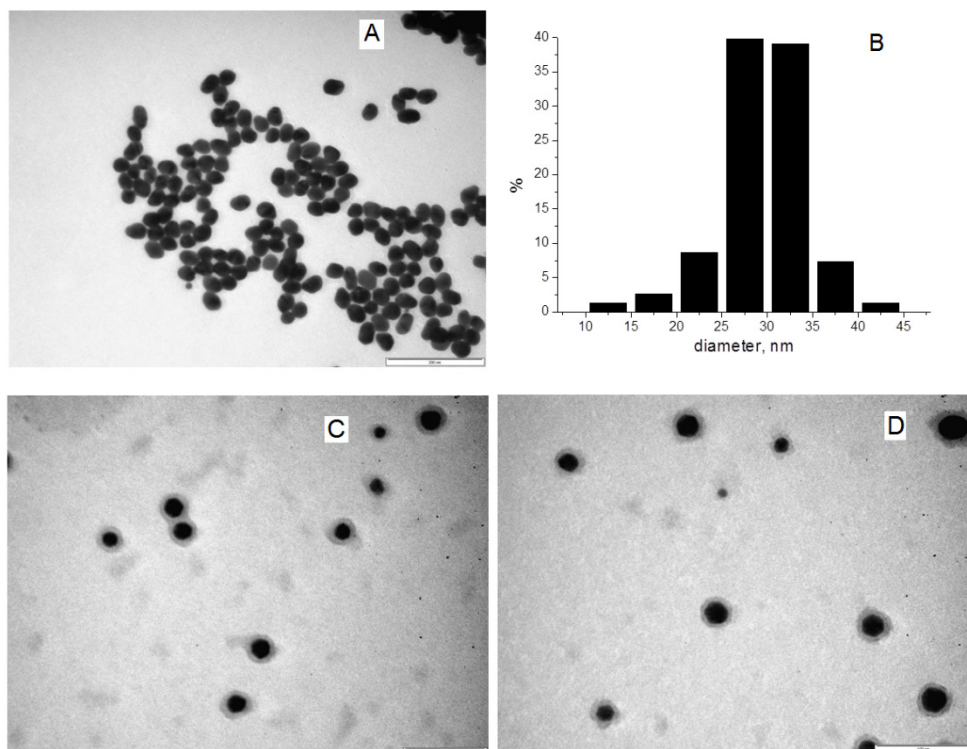
Figure 2. TEM image for synthesized GNP_C nanoparticles; the bar is 200 nm (panel A). Histogram of size distribution for GNP_C (panel B). TEM images for functionalized GNPs, used in sample 3 (Fig. 7) and sample 2 (Fig. 8), containing GNP-C 3.9 µg/mL, P 0.67 µg/mL (panel C), and for sample 4 (Fig. 7) and sample 3 (Fig. 8) containing GNP-C/A 3.9 µg/mL, D 0.21 µg/mL (panel D): the bar is 100 nm (panel C and panel D)

Figure 3 displays the morphology of the GNP-C layer adsorbed on glass from aqueous dispersion. The AFM images: 2D-topography image (A), phase image (B) and 3D-topography image (C) were obtained with atomic force microscope, operated in tapping mode. The nanoparticles of gold covered and stabilized by a layer of citrate, GNP_C, are well identified in every AFM image and they are well spread as a layer on glass showing a

rather small value of the surface roughness. However, the aggregated nanoparticles are also observed, particularly in the 3D-topography, where the height (the thickness of the GNP_C layer is rather high (about 56 nm), in comparison with the averaged diameter (around 30 nm) of NPs determined by TEM images. This aggregation might be related to a tendency of the formation of a double layer on GNP_C due to self-assemblies generation during the adsorption and drying process.
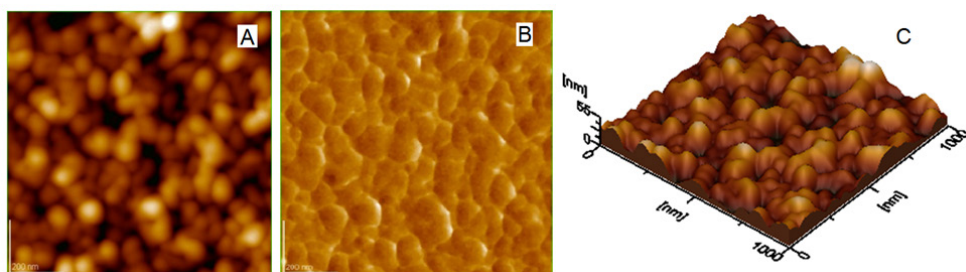
Figure 3. AFM images of gold nanoparticles synthesized and stabilized with citrate, GNP_C, as adsorbed layer on glass: 2D-topography (panel A); phase image (panel B); 3D-topography (panel C); scanned area 1 µm × 1 µm; surface roughness is given as root mean square, RMS, of about 4 nm

This situation might be caused by a strong interaction among the citrate covering layers on GNP_C justifying that the crystalline core of gold nanoparticle is very well covered by citrate layer as a stable shell.

The X-ray diffraction patterns for GNP are presented in Figure 4. Some characteristic peaks for gold are identified, at 2θ (^{o}) values: 38 (111 plane most intense signal); 44 (200); 65 (220); 78 (311). So, the presence of crystalline gold is evidenced. A peak also appears for NaCl, resulted from the synthesis reaction between $HAuCl_4$ and trisodium citrate ($Na_3C_6H_5O_7$).

The average size of GNP_C nanoparticles, obtained by Scherrer formula applied on the Au (111) diffraction peak in Figure 4, is about 15.6 nm, much smaller than the measured value by TEM images, given in Fig. 2. This is due to the fact that by XRD the size of crystalline domains is obtained within gold nanoparticles.

Adding positively charged doxorubicin (as water soluble doxorubicin hydrochloride, containing the cationic form of the therapeutic drug) to the negatively charged GNPs reduces their zeta-potential and thus, their stability against aggregation. For GNP_C, in the absence of a rather thick organic coating layer, the stability is mainly of electrostatic nature, thus we should

expect a significant destabilization of the aqueous colloidal system by doxorubicin, more important than for the GNP-R, already protected by a large layer of resveratrol [44]. The red color of the doxorubicin solution, due to its absorption band with a maximum at about 480 nm, is not visible at the low concentration used on cell lines, and does not interfere with the absorption band of the GNPs.
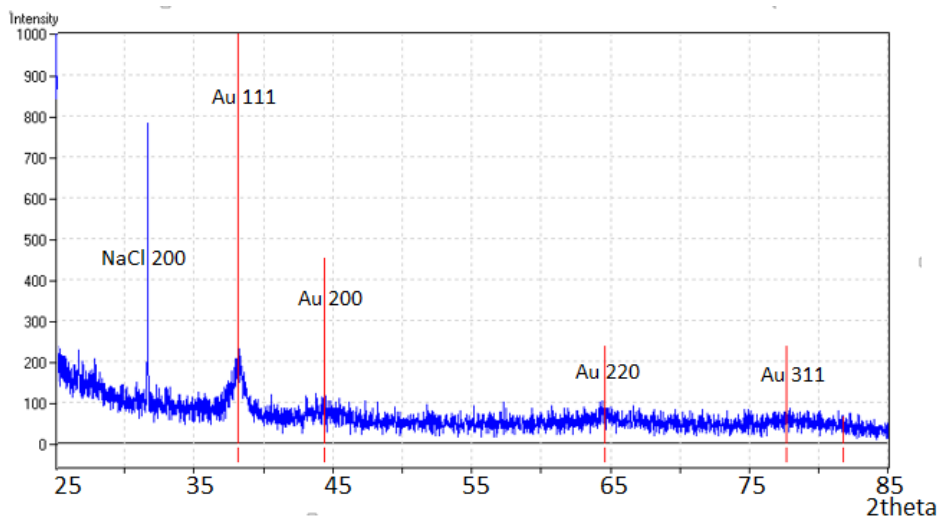

Figure 4. X-ray diffraction patterns for GNP_C nanoparticles. The red vertical bars give the positions of diffraction lines for crystalline gold domains

Therefore, GNP_C nanoparticles are highly sensitive towards the interaction with doxorubicin. Adding this compound, even in small amounts, changes almost immediately the color of the solution to violet and then to blue, followed by the sedimentation of GNPs aggregates. In the UV-Vis spectrum (Figure 5, panel A), the surface plasmon resonance, SPR, band characteristic for the GNPs is diminished and a new large band at higher wavelength (over 700 nm) appears, responsible for the change of color, and due to the formation of larger aggregates of particles. It is dominant both in the mixture 1 (mixt 1), of GNP_C and doxorubicin (D) solution (see Table 1) in the volume ratio 9:1 containing 106.2 mg/L Au and 4.2 mg/L D (mole ratio Au/D = 74/1, and flattens for a higher D content, as in mixture 2 (mixt 2) of the two solutions in the volume ratio 2:1, with: 78.7 mg/L Au; 14 mg/L D (mole ratio Au/D = 15.9/1), when the precipitation of the aggregates occurs.

The addition of resveratrol, R, solution, in the volume ratio GNP_C/R = 2:1 (Figure 5, panel B, mixture 3) does not affect the SPR band of GNP_C (black curve), while piperine, P, and icariin, Ic, solutions, in the same 2:1 v/v) ratio GNP_C/P (mixture 4) and respectively GNP_C/Ic (mixture 5) have both the same effect, a broadening and flattening of the GNP_C band. When doxorubicin is present, even in small amounts, together with resveratrol or piperine namely in the 5:4:1 volume ratio GNP_C: R: D (mixture 6), respectively GNP_C: P: Ic (mixture 7) of (Figure 5C), its effect is mostly the same as without R and P (Figure 5A).
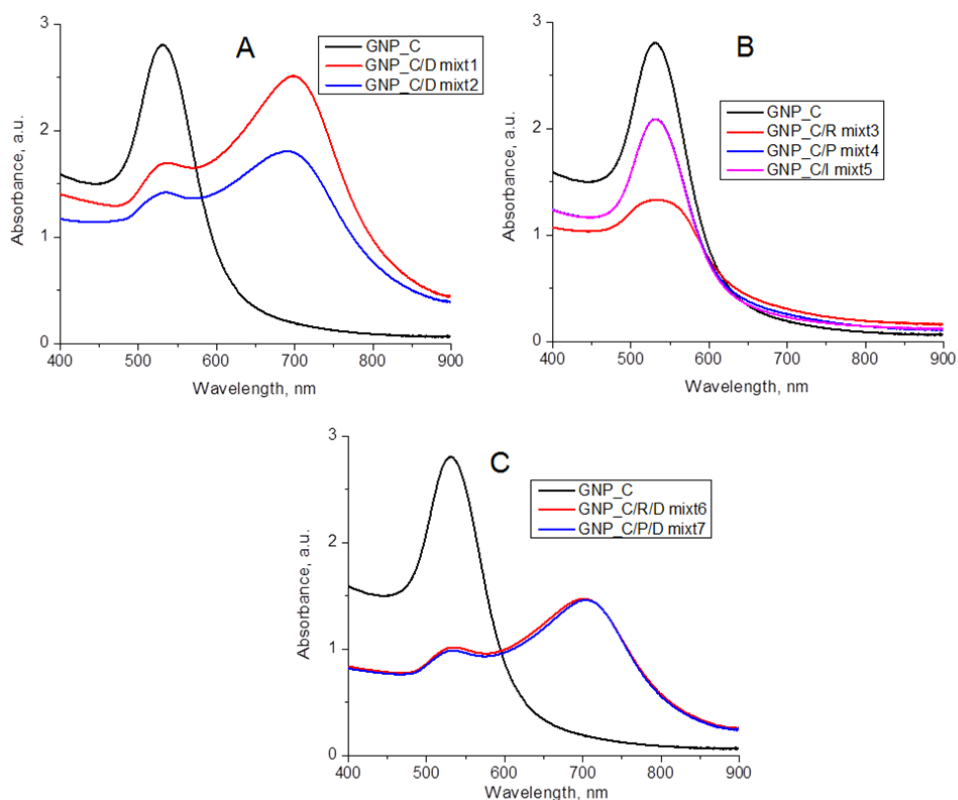
Figure 5. UV-Vis spectra of GNP_C (118 mg/L Au) mixtures with (panel A) doxorubicin (D), with contents (mg/L): mixt1: Au 106.2; D 4.2; mixt2: Au: 78.7; D 14 (B) resveratrol (R) - mixt 3: Au 39.3; R 10; piperine (P)- mixt 4: Au 78.7; P 13.3; and icariin (I)- mixt 5: Au: 78.7; I: 33.3; (C) resveratrol and doxorubicin – mixt6: Au 59; R 12; D 4.2; piperine and doxorubicin – mixt7: Au 58; P 10; D 4.2.

We had previously investigated the interaction between GNPs and asparagine, and found that asparagine binds to GNPs, resulting GNP_C/A nanoparticles, without causing their aggregation [4]. Therefore, we tried to protect the GNP_C against rapid aggregation by adding to their 0.6×10^{-3} mM colloidal solution a 10^{-3} M asparagine (A) solution. The colloidal GNP_C/A system is stable against increasing amounts of asparagine, from 20/1 to 2/1 v/v ratios of the two solutions (12/1 to 1.2/1 Au/A mole ratios) and also in time (Figure 6, panel A). By adding increasing volumes of doxorubicin solution (42 mg/L) to the GNP_C- asparagine 2/1 v/v mixture (named GNP_C/A), the colloidal GNP system is protected for a doxorubicin content up to 3.8 mg/L (volume ratio GNP_C/A/-D = 10/1), but the aggregation begins right away for 5.25 mg/L D (volume ratio GNP_C/A/-D = 7/1) and progresses rapidly in the first hour after mixing (Figure 6, panel B). It is to be noted that this instability appears in concentrated colloidal systems used in UV-Vis investigation. In the colloidal systems at low concentration of these biomolecules, as used in the cell culture, the stability of these diluted systems is highly increased for months, being deposited at 4 °C.
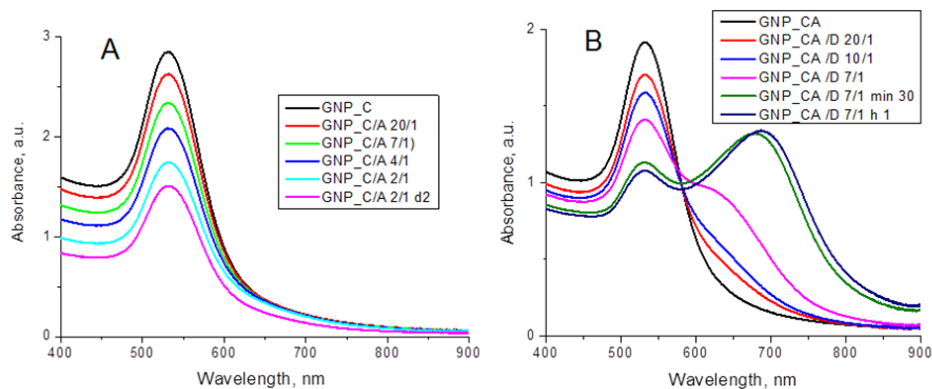
Figure 6. Panel A: UV-Vis spectra of 0.6 mM GNP_C solution at successive dilution with 10^{-3} M asparagine solution at the volume ratios given in figure, with an Au content (mg/L): 112.4 (20/1), 103.2 (7:1), 94.4 (4:1) and 78.7 (2:1), and after 2 days for the last solution. Panel B: Evolution of spectra of a solution containing GNP_C with asparagine (volume ratio 2:1 noted GNP_CA) at the addition of increasing volumes of doxorubicin (D) solution at the volume ratios GNP_CA/D given on figure: 20/1 (Au 75 mg/L, D 2 mg/L), 10/1 (Au 71.9 mg/L,D 3.82 mg/L,) and 7/1 (Au 68.9 mg/L; D 5.25 mg/L) and after 30 min and 1 h for the last mixture.

The functionalized GNP-C nanoparticles with piperine, as GNP_C 3.9 µg/mL, P 0.67 µg/mL, are shown in TEM image, Figure 2, panel C. The GNP-C nanoparticles stabilized with asparagine, A, and further functionalized with doxorubicin, as GNP_C/A 3.9 µg/mL, D 0.21 µg/mL, are presented in Figure 2, panel D. It is clear that the functionalized GNP_C nanoparticles are individually shown in TEM images, indicating in Figures 2C and 2D, an enhanced stability of these GNPs nanoparticles, in the experimental conditions without a clustering tendency. This is another good property of functionalized GNP_C nanoparticles, revealing that the agglomeration of these nanoparticles is not achieved under the experimental conditions. Moreover, the size of these functionalized GNP_C nanoparticles is close to the values of synthesized GNP_C nanoparticles (about 30 nm). AFM images of these functionalized GNP_C nanoparticles are revealing a similar nanostructure (not presented) as that shown in Figure 3.

Anticancer activity: cell viability and cytotoxic effects

In this study, we evaluated the cell viability and cytotoxic effect of GNP_C, also noted GNP-C (with 3.9 µg/mL, or with 19.83 µM, of tested AuNPs, sample 1, see Table 1), functionalized with resveratrol (0.5 µg/mL, sample 2), piperine (0.67 µg/mL, sample 3), as well as with very low doses of doxorubicin (0.21 µg/mL, sample 4) and icariin (1.67 µg/mL, sample 5) on the two breast carcinoma cell lines: MDA-MB-231 (in short MDA231) and MCF-7, as well as on tumor stem cells derived from glioblastoma (GM1) versus normal stem cells from the dental follicle (DF), treated with samples 1-4 (Table 2), by MTT assay. The MTT test shows cell viability depending on the cytotoxicity of an investigated compound. Cell viability was assessed after 24 hours of cells exposure to the chosen compounds. MTT solution (Sigma-Aldrich Chemicals GmbH, St. Louis, MO, USA) contains 3-(4,5-dimethylthiazolyl-2)-2,5-diphenyl tetrazolium bromide (which is a tetrazolium salt) that is reduced by mitochondrial enzymes active in viable cells. It results in a product, formazan, which is dark blue and is insoluble in aqueous solutions. The cells were incubated for another 1 h, and the formazan crystals were solubilized and the absorbance was measured by using a BioTek plate reader (see experimental part).

To perform the MTT viability test, MDA MB 231 cells and MCF-7 cells, as well DF stem cells and GM1 cells were seeded in 96-well plates and after 24 hours, when cells have adhered to the surface of the plate, the compounds to be studied were added in the concentrations indicated in Table1 and Table 2, respectively.

Table 1. Concentrations of tested compounds in µg/mL, and in µmol/L, for each sample (1 to 5) as well as mole ratios of Au/R, Au/P, Au/D and Au/Ic.

Samples (COMP)	Concentration		Mole ratios
	µg/mL	µmol/L	
1) GNP_C	Au 3.9	Au 19.83	-
2) GNP_C - R	Au 3.9; R 0.5	Au 19.83; R 2.2	Au/R 9.014
3) GNP_C - P	Au 3.9; P 0.67	Au 19.83; P 2.349	Au/P 8.442
4) GNP_C/A - D	Au 3.9; D 0.21	Au 19.83; D 0.36	Au/D 55.0
5) GNP_C - Ic	Au 3.9; Ic 1.67	Au 19.83; Ic 7.268	Au/Ic 2.728

The cells were treated with 19.83 µM of tested AuNPs and with chosen compounds given in Table 1, and after 24 h, the cell viability was determined by using MTT assay and the viable cells are given as % of Control, which is represented by untreated cells.

The graphic representation of the response of MDA MB 231 cells and MCF-7 cells to treatments with GNP-C, and GNP-C functionalized with resveratrol, piperine, and icariin, and GNP-C/A 3.9 µg/mL/ D 0.21 µg/mL, evaluated with the MTT viability test is given in Figure 7.

The two breast cancer lines, MDA MB 231 cells (in short MDA231) and MCF-7 cells were compared in terms of cell viability response to treatment with GNP_C (GNP-C) of 3.9 µg/mL of tested AuNPs, and further functionalized as following: GNP-C 3.9 µg/mL / R 0.5 µg/mL, GNP-C/R, GNP-C 3.9 µg/mL / P 0.67 µg/mL, GNP-C/P, GNP-C stabilized with asparagine (A), namely GNP-C/A 3.9 µg/mL / D 0.21 µg/mL (GNP-C/A/-D), GNP-C 3.9 µg/mL / Ic 1.67 µg/mL, GNP-C/Ic. Non-functionalized GNP-C showed a statistically significant toxicity (about 14 %) on breast cancer cell lines compared with untreated controls, with a reduction in the percentage of viable cells to 86% for MDA MB 231 and 84.6% for MCF-7. Functionalization with resveratrol (0.5 µg/ml), GNP-C/R, induced an important similar decrease in cell viability with an increase in cytotoxicity to 25% for both tumor lines. ($p<0.001$).

The functionalization of GNP-C with piperine, sample 3, GNP-C/P, and GNP-C/A/-D complex, sample 4, induced a decrease in viability for MDA231 cells with 30% and with 25% for MCF-7 cells. The introduction of icariin into GNP-C, sample 5, GNP-C/Ic dispersion had more intense effects for the MDA MB 231 cell line, with a decrease in cell viability to 73.6% compared to untreated cells. MCF-7 cells showed similar viability to cells treated with non-functionalized GNP-C, sample 1, upon treatment with GNP-C/Ic, sample 5.

The *t-test* concluded that the differences between GNP-C vs. GNP-C/R, vs. GNP-C/A/-D and vs. GNP-C/Ic are significant with a value of $p<0.05$* for MDA MB 231 cells. MCF-7 cells showed a more pronounced decrease in the values obtained for GNP-C / R compared to GNP-C (*t test* $p<0.05$*), and for the values of GNP-C/A/D vs. GNP-C ($p<0.01$**), see Figure 7.
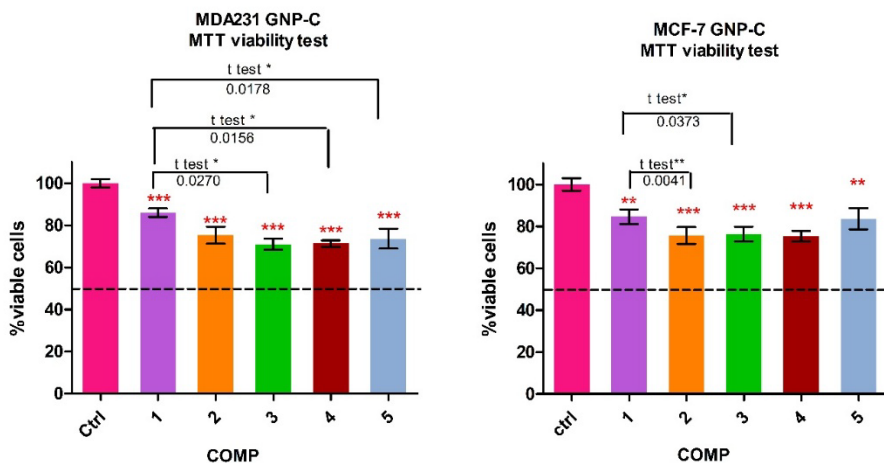
Figure 7. Cell viability (viable cells in % of Control (Ctrl), from MTT assay): Control (untreated cells); 1) GNP-C 3.9 µg/mL; 2) GNP-C 3.9 µg/mL, R 0.5 µg/mL; 3) GNP-C 3.9 µg/mL, P 0.67 µg/mL; 4) GNP-C/A 3.9 µg/mL, D 0.21 µg/mL; 5) GNP-C 3.9 µg/mL, Ic 1.67 µg/mL.

Two other cell types were also studied, the tumor stem cells isolated from a glioblastoma (GM1 cells) and the normal mesenchymal stem cells derived from the dental follicle (DF) to evaluate the possible antitumor effect of GNP-C functionalized or not, but also to ascertain the effects on normal cells. The stem cell lines were compared as response to treatment with GNP-C 3.9 µg/mL, sample 1, and functionalized with piperine (GNP-C 3.9 µg/mL/ P 0.67 µg/mL), sample 2, very low dose of doxorubicin (GNP-C/A 3.9 µg/mL / D 0.21 µg/mL), sample 3, and icariin (GNP-C 3.9 µg/mL / Ic 1.67 µg/mL), sample 4; the concentrations and mole ratios are noticed in Table 2.

Table 2. Type of composites, the concentration in µg/mL, and in µmol/L, for each sample (1-4) and mole ratios of Au/P, Au/D and Au/Ic.

Samples (COMP)	Concentrations		Mole ratios
	µg/mL	µmol/L	
1) GNP_C	Au 3.9	Au 19.83	-
2) GNP_C - P	Au 3.9; P 0.67	Au 19.83: P 2.349	Au/P 8.442
3) GNP_C/A - D	Au 3.9; D 0.21	Au 19.83: D 0.36	Au/D 55.0
4) GNP_C - Ic	Au 3.9; Ic 1.67	Au 19.83; Ic 7.268	Au/Ic 2.728

Graphic representation of the response of normal DF stem cells and GM1 glioblastoma tumor stem cells to treatments with GNP-C, sample 1, and with GNP-C functionalized with piperine, GNP-C/P, sample 2, and GNP-C/A 3.9 µg/mL/ D 0.21 µg/mL, sample 3, GNP-C/A/D, and with icariin, GNP-C/Ic, sample 4, evaluated with the MTT assay and viability test is given in Figure 8.

The obtained results showed a higher sensitivity of GM1 tumor stem cells to GNP-C, sample 1, treatments, with a 12.4% decrease in cell viability, in contrast to normal DF stem cells that were not affected by GNP-C administration. The functionalization of GNP-C with piperine (sample 2) and with icariin (sample 4) determined an increase in cytotoxicity by 6-8% compared to non-functionalized GNP-C (sample 1) in the case of GM1 cells, with a significant statistical difference at the t test ($p < 0.05$* for GNP-C vs. GNP-C/P; $p < 0.005$** for GNP-C vs. GNP-C/A/D. A similar response but of a lower intensity was also observed for normal DF stem cells. The effect of GNP-C functionalized with icariin, GNP-C/Ic, was gentler, with cell viability values of 88.2% for normal DF stem cells, than for GM1 tumor cells, showing a bigger decrease to 81% in cell viability (Figure 8).
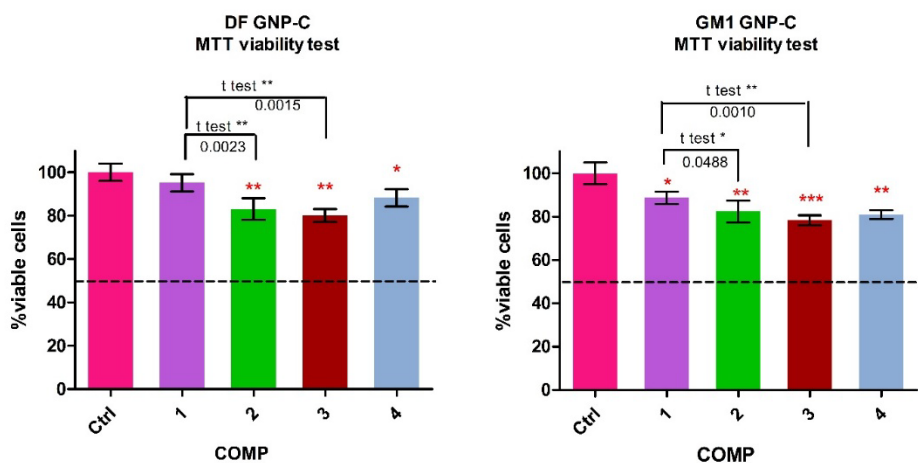
Figure 8: Cell viability (viable cells in % of Control, from MTT assay): Control (Ctrl); 1) GNP-C 3.9 µg/mL; 2) GNP-C 3.9 µg/mL / P 0.67 µg/mL; 3) GNP-C/A 3.9 µg/mL/ D 0.21 µg/mL; 4) GNP-C 3.9 µg/mL / Ic 1.67 µg/mL

The concentration of loaded bioactive molecules was very low in our study: for resveratrol 2.20 µmol/L, piperine 2.35 µmol/L, doxorubicin 0.36 µmol/L and for icariin 7.27 µmol/L, as shown in Table 1. GNP-C induced for all cells a reduced cytotoxicity, higher for breast cancer lines especially for hormone-dependent MCF-7 cells. Resveratrol loaded gold nanoparticles

have very similar effects on both breast cancer cell lines, in accordance with *Park et al. (2016)* study [46], which established that doses of 10 μM were non-toxic to MCF-7 breast cancer cells. The authors still reported that resveratrol-AuNPs showed better anti-invasive activity than resveratrol without cytotoxicity [43]. In a study conducted by *Wang et al. (2017)* [47]*,* MDA-MB-231 cells treated with free resveratrol and resveratrol-loaded solid lipid nanoparticles found that both treatments inhibited cell viability in a dose-dependent manner.

In present study, GNP-C loaded with piperine and with doxorubicin induced a more intensive cytotoxic effect against MDA231 cells compared with MCF-7 cells. The molar ratios between Au and biocompounds and doxorubicin chosen in this study (Au/R-9.014; Au/P-8.442; Au/D-55.0; Au/ic-2.728) showed that the presence of gold in these formulations determined the efficient internalization of biocompounds and doxorubicin, which even in very low concentrations managed to exert their influence on the cellular response with the inhibition of proliferation and the triggering of cell death mechanisms. The clinical applications of these functionalized nanoparticles with biocompounds are materializing in lowering the doses of cytostatic agents by sensitizing tumor cells to chemotherapeutics [48].

The glioblastoma tumor stem cells showed a higher sensitivity to GNP-C, GNP-C functionalized with piperine, GNP-C/P, or with doxorubicin, GNP-C/A/D, and icariin, GNP-C/Ic, treatments with an increase in cytotoxicity in contrast to normal stem cells, DF, that were not affected by GNP-C administration. Cancer stem cells show characteristics close to normal DF stem cells, with a hyper-glycolytic metabolism (Warburg effect) and lowered mitochondrial respiration, compared to more differentiated cells.

The strategies to target cancer stem cells are different from conventional therapies, inhibiting their self-renewal and chemoresistance-related pathways, or inducing their differentiation. Promoting glioma cancer stem cells (GSCs) differentiation is a strategy to improve therapeutic efficacy, using bioactive phyto-compounds that reduce self-renewal and tumor forming capacity, eliciting differentiation of primary glioma-derived stem cells; also, glioma tumor stem cells might be targeted by impairing their metabolism [49]. Differentiated glioblastoma multiform (GBM) cells, compared to cancer stem cells are more sensitive to temozolomide (TMZ) treatment. *Jeong S. et al* (2020) [50] demonstrated that piperine alone at doses between 1- 200 μM inhibited temozolomide-resistant human glioma cell growth, similar to TMZ. Association of piperine with low concentration of TMZ induced apoptosis by activation of caspase-8/-9/-3, MMP loss, and inhibition of cell migration [50]. Piperine can also have a radio-sensitizing effect in micromolar concentrations in the human glioma cells [51]. In our experiments, GNP_C (GNP-C) functionalized

with piperine (GNP-C/P) or with doxorubicin (GNP-C/A/D) induced the more intensive cytotoxic response in glioblastoma (GM1) stem cells (Figure 8), thus adding the piperine or doxorubicin to gold nanoparticles enhances their effects sensitizing the cells to these treatments.

CONCLUSIONS

The optimization of the GNPs functionalization and their concentration for loading various biomolecules to their site of action is of paramount importance and specific for every type of human cancer cell line. Moreover, cytotoxicity effectiveness plays a critical role in determining their practical utility, for potential medical applications, having also a high biocompatibility with living normal cells, while in targeting cancer cells inducing apoptosis. Additionally, this study highlights the characterization techniques for GNPs, their functionalization using biomolecules, and their potential applications in cancer therapy, emphasizing their potential in advancing therapeutic strategies.

EXPERIMENTAL SECTION

Material and methods

Materials

We prepared gold nanoparticles, GNP_C (symbolized also as GNP-C), by the reduction of tetrachloroauric acid, $(HAuCl_4 \cdot 3H_2O)$ 99.5% (Merck - Darmstadt, Germany), with trisodium citrate $Na_3C_6H_5O_7 \cdot 2H_2O$ (obtained from Sigma-Aldrich, Buchs, Switzerland). For the functionalization of GNP-C particles, anticancer biocompounds were used, namely: doxorubicin hydrochloride, D, (about 98%) from Sigma-Aldrich Chemie GmbH (Munich, Germany), trans-resveratrol, R, ≥ 99% (HPLC assay), from Sigma-Aldrich, (Buchs, Switzerland), piperine, P, ≥98% (HPLC assay), from AlfaAesar (Karlsruhe, Germany) and icariin, Ic, analytical standard (≥94%) from Sigma-Aldrich (Steinheim, Germany). Aqueous solutions were prepared with bidistilled deionized water. For the solubilization of icariin, dimethyl sulfoxide (DMSO) from Sigma-Aldrich (Schnelldorf, Germany) was used. Dulbecco's phosphate buffered saline (PBS), without $CaCl_2$ and $MgCl_2$, (pH 7.4), was necessary for the solutions used in cell cultures studies: it was purchased from AlfaAesar (Karlsruhe, Germany). We tried to stabilize the GNP_C solution against doxorubicin using the α-amino acid asparagine (Sigma-Aldrich, Steinheim, Germany).

Cell lines

Two breast cancer cell lines with different phenotypes / genotypes and different behaviors in terms of resistance to therapy were also tested: MDA-MB-231 (in short MDA231) and MCF-7, cell lines. Both human cell lines are derived from invasive ductal carcinoma. The MDA MB 231 cells are epithelial-type breast adenocarcinoma, negative for hormone receptors (triple negative) and with important mutations of anti-apoptotic protein p53. The lack of hormone receptors makes this cell line resistant to anti-hormonal therapies, but also to anticancer drugs [52, 53]. The MCF-7 line expresses estrogen receptors and are hormone-dependent [52]. Another particularly aggressive oncological localization was approached by performed tests on a line of tumor stem cells isolated from glioblastoma (GM1). The isolation method and the morphological and genetic characteristics, as well as the resistance to classical therapies were presented by *Tomuleasa et al (2010)* [39]. To evaluate the effect of gold nanoparticles on normal cells, stem cells derived from the dental follicle (DF) were used, which showed the phenotypic and functional characteristics of adult mesenchymal cells.

MDA MB 231 and MCF-7 (purchase from ATCC cell bank), glioblastoma GM1 cells and dental follicle (DF) stem cells were cultured in standard conditions. MCF-7 cells were cultured in Eagle's Minimum Essential Medium (MEM), supplemented with 10% fetal bovine serum (FCS), 2mM L-glutamine, 1% antibiotics, 1% non-essential amino acid solution (NEA). MDA MB 231 cells were cultured in RPMI-1640 medium supplemented with 10% fetal bovine serum (FCS), 2mM L-glutamine and 1% antibiotics. GM1 tumor stem cells derived from glioblastoma were cultured in DMEM medium with 4.5 g/L glucose, F12 HAM medium (DMEM / F12 1/1 ratio), with 10% fetal bovine serum (FCS), 1% antibiotics (penicillin and streptomycin), 2mM LGlutamine, 1% NEA, and DF cells were maintained in Dulbecco's modified Eagle's medium (DMEM) high glucose/F-12HAM (Sigma) containing 15 % fetal calf serum (FCS, Sigma), 2 mM L-Glutamine, 1 % antibiotics, 1 % non-essential aminoacids (NEA), 55 µM beta-mercaptoethanol, 1 mM natrium piruvate (all Sigma-Aldrich reagents).

Synthesis and functionalization of gold nanoparticles

In order to prepare the colloidal solution (dispersion) of GNP_C, 2 ml 1% (w/w) $HAuCl_4 \cdot 3H_2O$ aqueous solution (containing 0.05 mmol Au) was diluted with 80 ml ultrapure water, and 3 ml 1% aqueous trisodium citrate ($Na_3C_6H_5O_7 \cdot 2H_2O$) solution, (containing 0.1 mmol citrate) was added; the mixture was boiled for 1 minute, then cooled to room temperature. This dispersion was stable for years.

For the functionalization of the GNP_C nanoparticles, in colloidal dispersions, and the evaluation of their stability against aggregation and precipitation, they were mixed at various ratios with solutions of anti-cancer compounds. The solutions used in this investigation and their concentrations are given in Table 3. Since icariin is not soluble in water, it was solubilized in dimethyl sulfoxide (DMSO, 11 mg/10 ml) and then 100 ml PBS were added to that solution.

Table 3. Solutions used in this study

Solution	Solvent	Chemical formula	Molar mass (g/mol)	Concentration	
				mg/L	mmol/L
GNP_C	water	Au	197	118	0.6
Doxorubicin. HCl, D	water	$C_{27}H_{29}NO_{11} \cdot HCl$	580.0	42	0.072
Resveratrol, R	PBS	$C_{14}H_{12}O_3$	228.2	30	0.131
Piperine, P	PBS	$C_{17}H_{19}NO_3$	285.3	40	0.140
Icariin, Ic	DMSO, PBS	$C_{33}H_{40}O_{15}$	676.7	100	0.148
Asparagine, A	Water	$C_4H_8N_2O_3$	132.1	132	1

Characterization methods

*UV–Vis spectra (*190–900 nm wavelengths range) *were* measured with a Jasco UV–Vis V650 spectrophotometer (10 mm path length quartz cuvettes).

TEM images were recorded using JEOL standard software from a transmission electron microscope JEOL – JEM 1010. The GNPs colloidal dispersions were deposited on the carbon coated copper grids. After adsorption for 1 min the excess solution was removed with filter paper and the samples were air dried and ready for TEM examination.

AFM investigations were carried out on GNPs capped with citrate, GNP_C, as adsorbed layer (on glass plate) from the colloidal aqueous solutions for 10 s, washed with double distilled water and natural drying. Images were obtained using the AFM JEOL 4210 equipment, operated in tapping mode [5, 28], with standard cantilevers (resonant frequency 325 kHz, and spring constant 40 N/m) with silicon nitride tips. Scanned areas went from 10 μm × 10 μm to 0.5 μm × 0.5 μm on the same GNPs layer. The AFM images (2D- and 3D- topographies and phase images), were processed by the standard procedures with SPM2.0 processing software, JEOL, Japan.

Zeta- (ξ-) potential and *dynamic light scattering (DLS*) measurements were performed using the Malvern Zetasizer Nano-ZS90, on the colloidal gold solution.

X-Ray Diffraction (XRD) investigations were carried out using a Bruker D8 Advance diffractometer, in Bragg–Brentano geometry, equipped with a X-ray tube with copper target (K_α line, wavelength 1.541974 Å).

MTT viability assay

To perform the MTT viability test, MDA MB 231 cells, MCF-7 cells, DF stem cells and GM1 cells were seeded in 96-well plates at a cell density of 10^4 cells/well in 200 µL complete medium/well. After 24 hours, after the cells have adhered to the surface of the plate, the compounds to be studied were added in the concentrations indicated in Tables 1 and 2.

The MTT viability test was performed after 24 hours of exposure to the compounds using the tetrazolium salt (3-(4, 5-dimethylthiazolyl-2)-2, 5-diphenyltetrazolium bromide) (Sigma-Aldrich Chemicals GmbH, St. Louis, MO, USA). After removing the medium from the cell cultures, 100 µl of MTT solution (at concentration 1 mg/mL) was added to each well and after one hour of incubation at 37°C, in the dark, the MTT solution was discarded from the wells and added 150 µL of DMSO/well to solubilize the formazan crystals. Optical density, OD, readings were performed at 570 nm with a BioTek Synergy 2 microplate reader (Winooski, VT, USA). Each MTT assay determination was performed in triplicate.

Obtained OD values were then calculated as reported percentages of the control value (untreated cells of 100% cell viability), see Figures 7 and 8.

For the statistical analysis, GraphPad Prism 5 software was used, with the application of two statistical analysis methods: *firstly*, *one-way ANOVA* followed by the *"Dunnett multiple comparison test"* in which the optical density values obtained from untreated (control) cells were compared with OD values of cells treated with the compounds; *secondly, t test* applied for comparing two selected samples. Significant values were set at a $p < 0.05$ (*).

ACKNOWLEDGMENTS

REFERENCES

1. R. L. Siegel; A. N. Giaquinto; A. Jemal; *CA Cancer J. Clin.*, **2024**, *74*, 12–49
2. K. Sztandera; M. Gorzkiewicz; B. Klajnert-Maculewicz; *Mol. Pharmaceutics*, **2019**, *16*, 1−23
3. H. Huang; R. Liu; J. Yang; J. Dai; S. Fan; J. Pi; Y. Wei; X. Guo; *Pharmaceutics*, **2023**, *15*, 1868
4. O. Horovitz, A. Mocanu, G. Tomoaia, M. Crisan, L.-D. Bobos, Cs. Racz, M. Tomoaia-Cotisel, *Studia Univ. Babes-Bolyai, Chem*., **2007**, *52* (3), 53-71
5. G. Tomoaia; O. Horovitz; A. Mocanu; A. Nita; A. Avram; C. Pal Racz; O. Soritau; M. Cenariu; M. Tomoaia-Cotisel; *Colloids Surf. B Biointerfaces*, **2015**, *135*, 726-734
6. A. Sobczak-Kupiec; D. Malina; M. Zimowska; Z. Wzorek; *Digest J. Nanomater. Biostruct.*, **2011**, *6*(2), 803-808
7. A. Jakhmola; V. Onesto; F. Gentile; F. M. Kashkooli; K. Sathiyamoorthy; E. Battista; R. Vecchione; K. Rod; M. C. Kolios; J. (Jahan) Tavakkoli; P. A. Netti; *Mater. Today Sustain.*, **2024**, *28*, 101012
8. M. M. Khalaf; F. F. El-Senduny; H. M. A. El-Lateef; H. Elsawy; A. H. Tantawy; S. Shaaban; *J. Mol. Liq.*, **2021**, *340*, 117202
9. J. Dong; P. L. Carpinone; G. Pyrgiotakis; P. Demokritou; B. M. Moudgil; *Kona Powder Part. J.*, **2020**, *37*, 224-232
10. J. Piella; N. G. Bastus; Victor Puntes; *Chem. Mater.*, **2016**, *28*, 1066−1075
11. N. Hanzic; T. Jurkina; A. Maksimovic; M. Gotic; *Radiat. Phys. Chem.*, **2015**, *106*, 77-82
12. J.-W. Park; J. S. Shumaker-Parry; *J. Am. Chem. Soc.*, **2014**, *136*, 1907−1921
13. A. G. Memon; I. A. Channa; A. A. Shaikh; J. Ahmad; A. F. Soomro; A. S. Giwa; Z. T. Baig; W. A. Mahdi; S. Alshehri; *Crystals*, **2022**, *12*, 1747
14. L. Shi; E. Buhler; F. Boue; F. Carn; *J. Colloid Interface Sci.*, **2017**, *492*, 191-198
15. A. Tirkey; P. J. Babu; *Sens. Int.*, **2024**, *5*, 100252
16. D. Luo; X. Wang; C. Burda; J. P. Basilion; *Cancers*, **2021**, *13*, 1825
17. R. Z. Cer; U. Mudunuri; R. Stephens; F. J. Lebeda; *Nucl. Acids Res.*, **2009**, *37*, W441–W445
18. M. M. Fathy; A. A. Elfiky; Y. S. Bashandy; M. M. Hamdy; A. M. Elgharib; I. M. Ibrahim; R. T. Kamal; A. S. Mohamed; A. M. Rashad; O. S. Ahmed; Y. Elkaramany; Y. S. Abdelaziz; F. G. Amin; J. I. Eid; *Sci. Rep.*, **2023**, *13*, 2749
19. C. Freese; C. Uboldi; M. I. Gibson; R. E. Unger; B. B. Weksler; I. A. Romero; P.-O. Couraud; C. J. Kirkpatrick; *Part. fibre toxicol.*, **2012**, *9*, 23
20. D. Kumar; I. Mutreja; K. Chitcholtan; P. Sykes; *Nanotechnology,* **2017**, *28*(47), 475101
21. V. Raji; J. Kumar; C. S. Rejiya; M. Vibin; V. N. Shenoi; A. Abraham; *Exp. Cell Res.*, **2011**, *317*, 2052-2058
22. J. C. Mohan; G. Praveen; K.P. Chennazhi; R. Jayakumar; S.V. Nair; *J. Exp. Nanosci.,* **2015**, *8*(1), 32-45

23. S. Y. Choi; S. Jeong; S. H. Jang; J. Park; J. H. Park; K. S. Ock; S. Y. Lee; S.-W. Joo; *Toxicol. In Vitro*, **2012**, *26*, 229-237
24. J. Lee; D. K. Chatterjee; M. H. Lee; S. Krishnan; *Cancer Lett.*, **2014**, *347*, 46-53
25. S. K. Surapaneni; S. Bashir; K. Tikoo; *Sci. Rep.*, **2018**, *8*, 12295
26. E. E. Connor; J. Mwamuka; A. Gole; C. J. Murphy; M. D. Wyatt; *Small*, **2005**, *3*, 325-327
27. N. Tlotleng; M. A. Vetten; F. K. Keter; A. Skepu; R. Tshikhudo; M. Gulumian; *Cell. Biol. Toxicol.*, **2016**, *32*(4), 305-321
28. O. Horovitz; G. Tomoaia; A. Mocanu; T. Yupsanis; M. Tomoaia-Cotisel; *Gold Bull.,* **2007**, *40*(4), 295-304
29. M. A. Ujica; C.-T. Dobrota; G. Tomoaia; A. Mocanu; C.-L. Rosoiu; I. Mang, V. Raischi, M. Tomoaia-Cotisel; *Acad. Rom. Sci. Ann. Ser. Biol. Sci.*, **2024**, *13*(2), 145-167.
30. D. Delmas; V. Aires; E. Limagne; P. Dutartre; Frederic Mazue; F. Ghiringhelli; N. Latruffe; *Ann. N. Y. Acad. Sci.*, **2011**, *1215*, 48-59
31. J. J. Johnson; M. Nihal; I. A. Siddiqui; C. O. Scarlett; H. H. Bailey; H. Mukhtar; N. Ahmad; *Mol. Nutr. Food Res.*, **2011**, *55*, 1169–1176
32. J. K. Tak; J. H. Lee; J.-W. Park; *BMB reports*, **2012**, *45*(4), 242-246
33. Z. Jiang; K. Chen; L. Cheng; B. Yan; W. Qian; J. Cao; J. Li; E. Wu; Q. Ma; W. Yang; *Ann. N.Y. Acad. Sci*, **2017**, *1403*, 59-69
34. O. Vesely; S. Baldovska; A. Kolesarova; *Nutrients*, **2021**, *13*, 3095
35. S. Benayad; H. Wahnou; R. El Kebbaj; B. Liagre; V. Sol; M. Oudghiri; E. M. Saad; R. E. Duval; Y. Limami; *Cancers*, **2023**, *15*, 5488
36. Z. Bi; W. Zhang; X. Yan; *Biomed. Pharmacother.*, **2022**, *151*, 113180
37. Z. Yu; J. Guo; M. Hu; Y. Gao; L. Huang; *ACS Nano*, **2020**, *14*, 4816-4828
38. Z. Wang; L. Yang; Y. Xia; C. Guo; L. Kong; *Biol. Pharm. Bull.*, **2015**, *38*(2), 277-284
39. C. Tomuleasa; O. Soritau; D. Rus-Ciuca; H. Ioani; S. Susman; M. Petrescu; T. Timis; D. Cernea; G. Kacso; A. Irimie; I. S. Florian; *J. Buon.*, **2010**, *15*(3), 583-591
40. R. Cailleau; R. Young; M. Olive; W. J. Reeves Jr.; *J. Natl. Cancer. Inst.*, **1974**, *53*(3), 661-674
41. R. Watkins; L. Wu; C. Zhang; R. M. Davis; B. Xu; *Int. J. Nanomedicine*, **2015**, *10*, 6055-6074
42. K. de Vries; M. Strydom; V. Steenkamp; *J. Herb. Med.*, **2018**, *11*, 71-77
43. V. Sanna; N. Pala; G. Dessi; P. Manconi; A. Mariani; S. Dedola; M. Rassu; C. Crosio; C. Iaccarino; M. Sechi; *Int. J. Nanomedicine*, **2014**, *9*, 4935-4951
44. M. A. Ujica; I. Mang; O. Horovitz; A. Mocanu; M. Tomoaia-Cotisel; *Studia Univ. Babes-Bolyai, Chem.,* **2025**, *70* (1), 47-63
45. R. J. Hunter, *Zeta Potential in Colloid Science: Principles and Applications*, Academic Press, London, **1981**, pp. 363-369
46. S. Y. Park; S. Y. Chae; J. O. Park; K. J. Lee; G. Park; *Oncol. Rep.*, **2016**, *35*(6), 3248-3256
47. W. Wang; L. Zhang; T. Chen; W. Guo; X. Bao; D. Wang; B. Ren; H. Wang; Y. Li; Y. Wang; S. Chen; B. Tang; Q. Yang; C. Chen; *Molecules*, **2017**, *22*(11), 1814
48. Hakeem AN; El-Kersh DM; Hammam O; Elhosseiny A; Zaki A; Kamel K; Yasser L; Barsom M; Ahmed M; Gamal M; Attia YM; *Sci Rep*. **2024,** *14*,18181

49. F. Pistollato; S. Bremer-Hoffmann; G. Basso; S. S. Cano; I. Elio; M. M. Vergara; F. Giampieri; M. Battino; *Targ. Oncol.*, **2016**, *11*(1),1-16
50. S. Jeong; S. Jung; G. S. Park; J. Shin; J. W. Oh; *Bioengineered*, **2020**, *11*(1), 791-800
51. S. Diehl; G. Hildebrandt; K. Manda; *Int. J. Mol. Sci.*, **2022**, *23*(15), 8548
52. T. A. Theodossiou; M. Ali; M. Grigalavicius; B. Grallert; P. Dillard; K. O. Schink; C. E. Olsen; S. Walchli; E. M. Inderberg; A. Kubin; Q. Peng; K. Berg; *NPJ Breast Cancer*, **2019**, *5*, 13
53. Y. Li; S. Upadhyay; M. Bhuiyan; F. H. Sarkar; *Oncogene*, **1999**, *18*(20),3166-3172